

Transient nucleate boiling under stepwise heat generation for highly wetting fluids

Marie-Christine Duluc^a, Benoit Stutz^b, Monique Lallemand^{b,*}

^a LIMSI-CNRS, UPR 3251, B.P. 133, 91403 Orsay Cedex, France

^b Centre de Thermique de Lyon, UMR CNRS 5008, INSA, 20 av. Albert Einstein, 69621 Villeurbanne Cedex, France

Received 15 February 2004

Available online 16 September 2004

Abstract

Experiments of transient nucleate boiling are carried out on highly wetting fluids from two metallic specimen, a thick flat sample and a wire. The initial condition is controlled in terms of the system temperature as well as by a primary activation of the nucleation sites. A stepwise heat generation is investigated and the role of thermal inertia is clarified. The thermal behaviour of the system and the associated time scales are found to depend on temperature at boiling inception. This one is similar to the steady-state value for the thick flat sample but depends on the magnitude of the heating step in the case of the thin wire.

© 2004 Elsevier Ltd. All rights reserved.

Keywords: Transient boiling; Stepwise heat generation; Thermal inertia; Onset boiling

1. Introduction

The comprehension of transient boiling mechanisms is an important challenge because transient phenomena are commonly encountered in practical applications. For instance, considering the starting of a boiling system, heat transfer has to be controlled in order to avoid any unwanted superheat during the transient process that could deteriorate heat transfer or damage the system.

Even though realistic situations generally involve systems of high thermal inertia, few transient pool boiling

experiments were developed with large heat capacity samples. Auracher and Marquardt [1] have investigated transient pool boiling from a thick copper sample with FC 72. In their experiments, all the nucleation sites are activated at the start of the heating. They observed a hysteresis between heating transient conditions (up to 50 K s^{-1}) and cooling (up to 4 K s^{-1}): heat flux increases (decreases) strongly with increasing (decreasing) heating rate. Under steady boiling conditions, with a clean heater surface, no hysteresis was observed. Héas et al. [2] performed pool boiling experiments with a thick copper sample and pentane in saturated conditions. This investigation clearly showed that temperature at boiling incipience as well as the measurement reproducibility strongly depend on boiling incipience conditions. Parameters such as the initial temperature of the surface and the waiting period between the preliminary procedure and the heat input seem to control the presence

* Corresponding author. Tel.: +33 4 72 43 81 54; fax: +33 4 72 43 60 10.

E-mail address: monique.lallemand@insa-lyon.fr (M. Lallemand).

Nomenclature

α	thermal diffusivity, m^2s^{-1}
D	wire diameter, m
g	acceleration due to gravity, ms^{-2}
h	heat transfer coefficient, $\text{Wm}^{-2}\text{K}^{-1}$
h_{lg}	latent heat of vaporisation, Jkg^{-1}
I	electric current, A
J	rate of nuclei formation per unit volume, $\text{m}^{-3}\text{s}^{-1}$
k_B	Boltzmann constant $1.3805 \times 10^{-23} \text{JK}^{-1}$
L	wire length, m
m	mass of one molecule, kg
\bar{N}	number of molecules per unit volume, m^{-3}
p	pressure, Pa
q''	heat flux, Wm^{-2}
q^*	dimensionless heat flux supplied to the heating element = $(q'' - q''_{\text{ONB}})(q''_{\text{CHF}} - q''_{\text{ONB}})$
Q	energy stored in the heater, J
\mathfrak{R}	electrical resistance of the wire, Ω
Ra	roughness, m
r_c	cavity radius, m
R_i	specific gas constant, $\text{Jkg}^{-1}\text{K}^{-1}$

t	time, s
T	temperature, K
U	voltage, V

Greek symbols

γ	temperature coefficient of the wire, ΩK^{-1}
δ	film thickness, m
δ_d	thermal diffusion distance, m
ΔT_{ONB}	wall superheat at boiling incipience, K
ΔT_w	wall superheat $\Delta T_w = T_w - T_{\text{sat}}$, K
ρ	density, kgm^{-3}
σ	surface tension, Nm^{-1}

Subscripts

char	characteristic
CHF	critical heat flux
g	vapour
l	liquid
ONB	onset boiling
sat	saturation
w	wall

of residual amount of gas in cavities. The superheat at boiling onset is related to the activation of entrapped gas. The energy supplied to the cartridge heaters, the one stored in the thick sample and the one transferred to the fluid have been investigated for the different stages of transient boiling.

The effect of wall material and surface conditions on the growth of the initial bubble of R-113 has been investigated by Okuyama et al. [3] using a large heat capacity sample. At boiling incipience, a vapour bubble appears on the heater and grows in a peculiarly straw-hat shape to cover the entire surface. The growth of this vapour structure is found to be the result of a lateral coalescence process between the vapour structure itself and small bubbles activated in succession around it along the heater surface. The growth rate of the straw-hat bubble depends on the surface roughness, which may affect the density of activated nuclei. Kawamura et al. [4] pointed out that the heat flux at the departure from nucleate boiling in transient boiling increases asymptotically up to a constant value, as test samples become thicker. This effect vanishes when the thickness of the test samples becomes larger than the thermal diffusion distance δ_d during the transient period ($\delta_d = \sqrt{\alpha_w t_{\text{char}}} \approx 0.3 \text{ mm}$ for a piece of stainless steel and a characteristic time of $t_{\text{char}} = 30 \text{ ms}$).

If only few results are available for large heat capacity samples, transient pool boiling on thin wires has been, on the other hand, widely investigated. This

is likely to be due to the simplified analysis on such a one-dimensional geometry. Various studies have been performed with several working fluids [5–13]. Attempts have been made to qualify the system for heating modes like heating steps [7–9,11,13], rampwise [10,11] or exponential heating [5,6,11,12]. Studies investigating the effect of a heating step in liquid nitrogen revealed that a premature transition to film boiling may be observed, i.e. for a heat flux lower than the critical heat flux. Sinha et al. [8] reported this kind of transition for heat fluxes as low as 40% of the peak heat flux, which was confirmed later on by Tsukamoto et al. [7]. Using a high speed video camera, Tsukamoto et al. [7] and Okuyama et al. [9] identified three different scenarii for this transition: at low heat fluxes, transition is due to coalescence of nucleate boiling bubbles. For intermediate heat fluxes, onset boiling occurs in the form of a vapour sheath that spreads along the heater until steady film boiling is established. Then for very high heat fluxes, numerous tiny bubbles are generated simultaneously on the heating element that finally coalesce and lead to steady film boiling. In this latter case, the wire temperature at boiling incipience reaches the homogeneous nucleation temperature. A very high heating step supplied on a thin wire may then be employed to measure temperature for homogeneous nucleation as formerly proposed by Sinha et al. [8], using liquid nitrogen under various pressures. All these investigations were performed with short recording

times because onset boiling occurs very quickly, generally in less than 0.1 s after the beginning of the heating step. Similar experiments performed with longer recording times [13] revealed that this premature transition may in some cases not be definitive. A few seconds is sometimes required for the system to achieve a steady nucleate boiling state. Heat transfer associated to a stepwise heating is first realised by conduction. Convection may be observed provided that the heat pulse is not too high.

Whatever was performed on thick flat samples or on thin wires, all these transient studies have shown that, similarly to steady conditions, a liquid superheat is required for boiling incipience and heat transfer is first realised in the single liquid phase. The prediction of temperature at boiling inception is far from being understood and represents the first challenge of these transient studies. A brief outline of boiling inception under steady-state conditions seems useful to be presented here. Onset boiling from a heated surface may be explained either by the heterogeneous nucleation theory or by the activation of entrapped gas or vapour in cavities. The heterogeneous nucleation is the formation of critical size nuclei within a metastable liquid phase at a solid–liquid interface, provided that there is no vapour or gas trapped in cavities at the beginning of the fluctuation process. The free energy of formation of a nucleus can be reduced in the presence of a solid surface [14]. This reduction depends on the surface geometry and on the contact angle between the liquid and the solid surface. A summary of analytical results on heterogeneous nucleation for different geometries has been provided for high contact angles by Thormählen [15]. An effective reduction of the superheat is found in comparison with the homogeneous nucleation theory. Conversely, for highly wetting fluids, homogeneous nucleation within the superheated fluid is more probable (to initiate boiling, heterogeneous nucleation requires a higher superheat than homogeneous nucleation), except for particular shapes of micropores. Therefore, onset boiling is generally attributed to the presence of entrapped gas or vapour in cavities. Bankoff [16] has considered the mechanism of vapour and liquid entrapment within cavities: the liquid–solid contact angle must be greater than twice the half cone for cavities to trap gas or vapour. Griffith and Wallis [17] proposed to determine temperature at boiling onset from the cavity mouth diameter. This corresponds to a minimum value of the curvature radius of the nucleus. Considering the Clausius–Clapeyron and the Laplace–Kelvin equations, an expression was derived to predict the cavity radius r_c , from which the bubble is generated at boiling incipience:

$$\Delta T_{\text{ONB}} = \frac{2\sigma T_w}{\rho_g h_g r_c} \quad (1)$$

Hsu [18] showed that boiling onset and the size of nucleation cavities strongly depend on the thickness of the liquid boundary layer surrounding a static vapour embryo. Assuming a linear temperature distribution in the thermal boundary layer, Hsu determined the maximum and minimum sizes of nucleation sites. Tong et al. [19] showed that the contact angle hysteresis (the dynamic contact angle is always greater than the static contact angle) may enhance vapour entrapment and thus may have a significant influence on boiling onset. Wang and Dhir [20] extended the criterion of Griffith and Wallis to include conical, spherical and sinusoidal cavities. They also observed experimentally that, for wetting fluids, most of the conical cavities present on the surfaces are not expected to nucleate [21]. Nucleation sites are believed to be reservoir-type cavities. They showed that, for wetting fluids (with contact angle less than 90°), the incipience superheat is independent of the contact angle and is thus predicted by the Griffith and Wallis criterion. Qi et al. [22] observed experimentally that only deep cavities satisfying the Bankoff's criterion, trap gas or vapour.

The purpose of the present paper is to investigate transient nucleate boiling under stepwise heat generation for highly wetting fluids. The influence of thermal inertia is also examined, using two different solids, a thick flat sample and a thin wire. In both cases, the initial condition is controlled by the means of two parameters: the system temperature and the presence of pre-existing vapour within cavities. The second condition is achieved by a preliminary heating procedure, implemented systematically before each run. The experimental set-up will first be described for both test samples as well as the primary procedure. In the next section, steady boiling curves obtained for both solid–fluid combinations will be presented and their own characteristics highlighted. In section 4, transient results will then be examined. A comparative analysis of transient feature for both samples will be outlined in the concluding section.

2. Experimental set-up and procedure

2.1. Thick flat sample

A schematic diagram of the experimental device is shown in Fig. 1 [2]. The pool-boiling vessel is a 160 mm inner diameter and 150 mm-height cylinder. A height of 90 mm of liquid is maintained above the boiling surface. Two chromel–alumel thermocouples are placed in the vessel to measure liquid and vapour temperatures. The test heater is a 90 mm height cylindrical copper block, isolated on its perimeter with Teflon. Two cartridge heaters are imbedded in the sample. The 30 mm diameter-boiling wall is horizontal and flushed with the vessel bottom. Noncondensable gases are

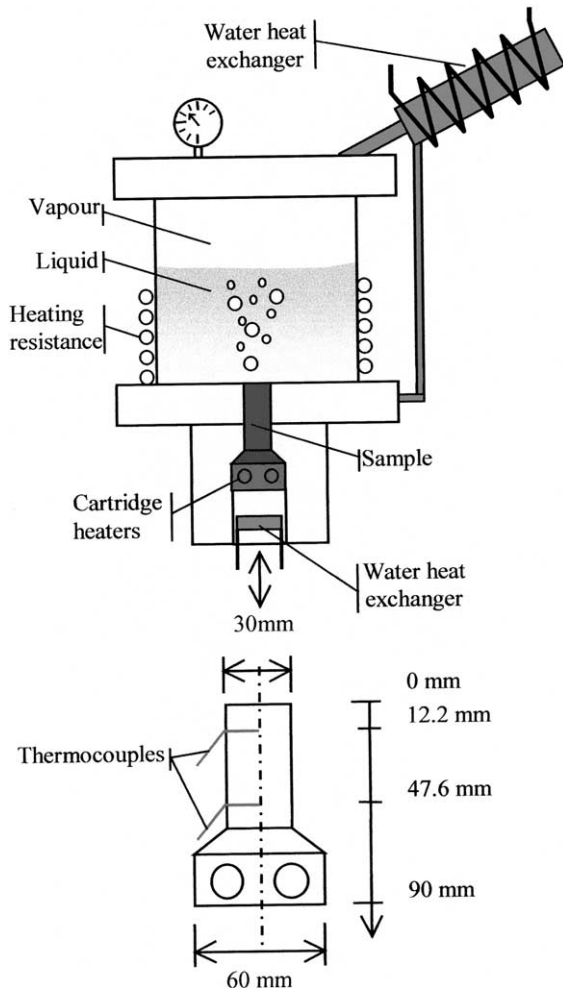


Fig. 1. Experimental set-up used to study transient nucleate boiling of the thick flat sample.

released using a vent on the top of the chamber. The pressure is maintained constant during the experiments using an external condenser and a heating resistance.

Two chromel–alumel thermocouples located at 12.2 and 47.6 mm beneath the surface are used to determine the heat flux and the wall temperature by mean of an inverse heat conduction method [23]. Uncertainty of the wall temperature due to the uncertainties in the thermocouple position, copper thermal properties and thermocouple calibration is around ± 0.2 K. The accuracy in surface heat flux is within ± 0.2 Wcm^{-2} for heat flux smaller than 5 Wcm^{-2} and within ± 0.5 Wcm^{-2} for higher heat flux. The data acquisition rate and thus the calculation rate of the surface heat flux and surface temperature superheat is 1 Hz. The experiments are performed using pentane as test liquid in saturated conditions at $p = 1$ atm ($T_{\text{sat}} = 36$ °C). The test surface is either a mirror finish or a rough surface. Roughness

characteristics of each heater surface obtained with an UBM technique have a Ra value less than 0.06 or 1 μm , respectively.

2.2. Wire

The wire is made of brass, 25 μm in diameter and 50 mm in length. It is connected horizontally on four supports: two for current input and two other ones for voltage measurement. The inner pins were designed with a large thermal inertia in order to control the boundary conditions ($T = T_{\text{sat}}$). The cell is immersed in a dewar filled up with liquid nitrogen. The cylindrical container is 150 mm in diameter and the liquid height above the wire is about 400 mm. A schematic diagram of the experimental apparatus is shown in Fig. 2. The experiments are performed using nitrogen under atmospheric pressure and saturation conditions (1 atm; 77.35 K). The thermoresistive nature of brass makes the wire both a heater and a thermometer. Its temperature coefficient is constant in the investigated temperature range and equal to 0.01 ΩK^{-1} . The heat flux dissipated by Joule effect $q''_j(t)$ and the average wire superheat $\Delta T_w(t)$ are determined as follows:

$$q''_j(t) = \frac{U(t)I(t)}{\pi DL} \quad (2)$$

$$\Delta T_w(t) = \bar{T}_w(t) - T_{\text{sat}} = \frac{1}{\gamma} \left(\frac{U(t)}{I(t)} - \Re(T_{\text{sat}}) \right) \quad (3)$$

$$\text{with : } \bar{T}_w(t) = \frac{1}{L} \int_0^L T(x, t) dx \quad (4)$$

The transient heating investigated in this work is a heating step. Due to the very small temperature coefficient of the wire, this is achieved by the means of a volt-

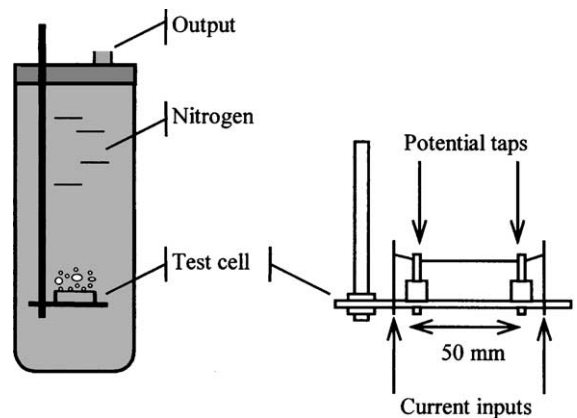


Fig. 2. Experimental set-up used to study transient nucleate boiling of the thin wire.

age step. Time evolution of the heat flux and the wire temperature are recorded by an acquisition system including two analogical differential amplifiers. Data acquisition is performed up to a sampling rate of 4000 Hz, the time skew between sampled channels being less than 50 ns. The whole experimental set-up leads to an uncertainty less than ± 0.5 K in temperature and ± 0.2 Wcm^{-2} in heat flux. More details about the experimental set-up are available elsewhere [13,24].

2.3. Preliminary procedure

Héas et al. [2] as well as Anderson and Mudawar [25] showed that time, temperature and pressure prior to transient boiling experiments greatly influence the onset of boiling and the temperature overshoot. A heating procedure, preliminary to any heating step, is therefore applied to ensure a good experimental reproducibility and to allow comparison of transient boiling results obtained from the two heating samples:

1. Heat flux is gradually supplied to the test heater in order to achieve a medium nucleate boiling state without risk of surface damage. The heat input is then increased up to 80% of the critical heat flux ($q''_{\text{CHF}} = 27 \text{ Wcm}^{-2}$ for the thick flat sample with pentane and 23 Wcm^{-2} for the wire with nitrogen). The heater surface is maintained in this vigorous boiling regime during a time long enough to ensure the activation of many nucleation sites (30 min for the thick flat sample and 0.5 min for the wire).
2. After that, the heating power is switched off. The wire, immersed in a large pool of liquid, recovers rapidly the saturation temperature. The thick flat sample is cooled down by a water heat exchanger located at its bottom until the wall temperature reaches the saturation value.
3. Before the heating step, a waiting period with no heat input is maintained during 5 min for both samples in order to stop any fluid motion induced by convection.
4. A stepwise input is applied to the wire and to the cartridge heaters, respectively.
5. A wall temperature increase is observed as a result of the heating step. For the wire, of very low thermal inertia, the heat flux released to the fluid is quite equal to the heating step and temperature variations as high as 2000 K s^{-1} are measured. For the thick flat sample, the energy supplied to the cartridge heaters during the free convection regime is quite equal to the energy stored in the solid due to the small heat transfer coefficient and the large thermal inertia of the test heater. Therefore, the heat flux released to the fluid is very low compared to the wire case. A transient heating up to 0.25 K s^{-1} is obtained.

3. Steady boiling curves

3.1. Thick flat sample

Fig. 3 shows the boiling curve obtained in stationary conditions for two samples of different surface roughness: a mirror finished surface ($Ra = 0.06 \mu\text{m}$) and a rough surface ($Ra = 1 \mu\text{m}$). The heat flux is increased with steps of about 0.5 Wcm^{-2} in the convective regime and about 2 Wcm^{-2} in nucleate boiling. The classical correlations, used to predict the average heat transfer coefficient in the case of free convection induced by an isothermal horizontal plate facing upwards (Mac Adams), are relevant with our experimental results.

At boiling incipience, the wall superheat ΔT_{ONB} is about 40 K and heat flux q''_{ONB} is close to 2.8 Wcm^{-2} . According to the Griffith and Wallis equation, this corresponds to a cavity mouth diameter of about $0.4 \mu\text{m}$. The exact value of the surface temperature at boiling incipience is very difficult to determine because vapour mostly occurs between two heating steps. It can be noticed that onset boiling in steady experiments is not significantly affected by the sample roughness. Conversely, for the nucleate boiling regime, heat transfer increases with the surface roughness and the boiling curve is shifted to the left. Moreover, for heat flux values lower than 21 Wcm^{-2} (about 80% of the critical heat flux), the slope of the boiling curve is higher for the smoothest surface. Beyond this point, heat transfer looks similar for both surfaces. This feature can be explained considering the distribution of nucleation sites over both surfaces: any increase of the wall superheat leads to the activation of smaller cavities and thus to a regular increase of the nucleation sites density. The distribution of cavity sizes appears to be quite different for the two samples: steady nucleate boiling on the rough surface is observed for wall superheats ranging between 12

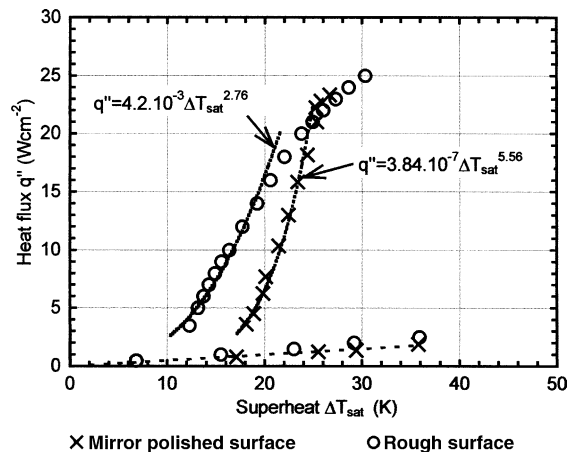


Fig. 3. Steady-state boiling curve of the thick flat sample.

and 30 K, which corresponds to nucleation sites of diameter included between 1.4 and 0.59 μm . The wall superheat is included between 18 and 30 K for the smooth surface, which corresponds to nucleation sites of diameter included between 0.94 and 0.59 μm . Then, in this latter case, the narrow distribution of active nucleation sites leads to a higher slope of the nucleate boiling curve.

The experimental critical heat flux measured for the mirror finish surface and the rough surface are respectively equal to 23 and 25 Wcm^{-2} . This is in good agreement with the critical heat flux of 27 Wcm^{-2} deduced from the Zuber-Kutadeladze model [26].

3.2. Wire

A steady boiling curve, obtained with the brass wire immersed in liquid nitrogen, is presented in Fig. 4. This geometry displays two main characteristics: natural convection is sustained to a high heat flux, nearly equal to one half of the critical heat flux ($q''_{\text{CHF}} = 23 \text{ Wcm}^{-2}$) and nucleate boiling develops along a quasi-vertical line.

Heat is transferred to the fluid by natural convection as long as vapour has not occurred on the surface. Boiling occurs for a wire superheat ΔT_{ONB} of about 18 K and a heat flux (q''_{ONB}) close to 9 Wcm^{-2} . Considering the Griffith and Wallis criterion given by Eq. (1), this superheat can be related to a cavity radius r_c nearly equal to 0.09 μm . This tiny value has to be connected to the small diameter of the wire, whose surface may be considered as a smooth one. For cylinders, natural convection heat transfer is enhanced when the diameter is reduced. This feature, combined with the high superheat required for boiling inception, gives an explanation to the curve presented in Fig. 4.

After boiling incipience, a small increase of the heat flux leads to a decrease of the wall superheat. Several points of that kind are observed until a heat flux value, nearly equal to 12 Wcm^{-2} , is achieved. These points,

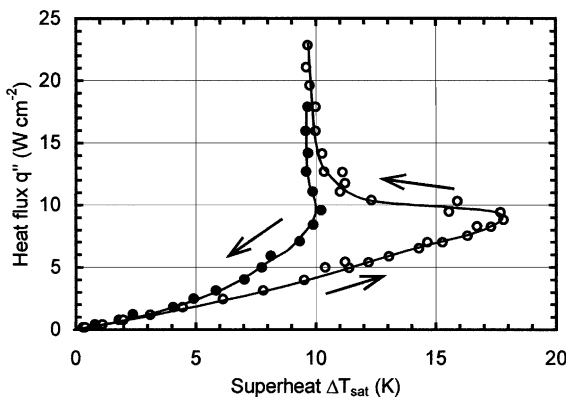


Fig. 4. Steady-state boiling curve of the wire.

that are not observed for decreasing heating steps, correspond to the gradual activation of the nucleation sites. The superheat presented on the boiling curve is a mean value, as given by Eqs. (3) and (4). A local decrease in the wire temperature, as one induced for instance by the activation of a few nucleation sites, leads to a decrease of the mean wire superheat.

Beyond a heat flux value equal to 12 Wcm^{-2} , nucleate boiling develops along a quasi-vertical line. This is due to the smoothness of the surface as formerly shown by Courty and Foust [27]. For this kind of surface, the size distribution of nucleation sites is narrow and any increase of the wire superheat is followed by the activation of many sites. Heat transfer is therefore of high efficiency. This feature is similar to the one observed on the thick flat sample with the smooth surface. In the case of a thin wire, forces that hold the bubble on the surface are reduced compared to the case of a flat plate. Hence, bubble diameter at lift-off is lower and coalescence (lateral or vertical) is postponed. The critical heat flux is therefore higher than for a flat plate. Since classical correlation derived from the Zuber model for flat plates is no longer relevant for very thin wires, a modified correlation was proposed by You et al. with an accuracy of about $\pm 20\%$ [28]:

$$\frac{q''_{\text{CHF}}}{q''_{\text{CHF,Z}}} \cong 0.89 + 1.01e^{-2.18\sqrt{R'}} \quad \text{for } R' > 0.0123 \quad (5)$$

R' being a dimensionless radius defined as:

$$R' = \frac{D/2}{\sqrt{\frac{\sigma}{g(\rho_l - \rho_g)}}} \quad (6)$$

and $q''_{\text{CHF,Z}}$ is the critical heat flux derived by Zuber for an infinite horizontal flat plate.

For liquid nitrogen, the $q''_{\text{CHF,Z}}$ value is about 16.3 Wcm^{-2} . The wire diameter used in the present investigation leads to a dimensionless radius R' of 0.0117, i.e. a little lower than the limiting value proposed by You et al. Reporting this quantity in Eq. (5), the critical heat flux predicted by this correlation is 27.5 Wcm^{-2} . The value measured in the present experiment is about 23 Wcm^{-2} , i.e. 15% lower. Hence, the correlation proposed by You et al. is still relevant for this R' value.

4. Transient nucleate boiling

In this section, transient results for the thick flat sample and the wire are presented and discussed.

4.1. Thick flat sample

A stepwise heat generation is supplied to the cartridge heaters. Therefore, heat flux transferred to the fluid is, at any time, the difference between the electrical

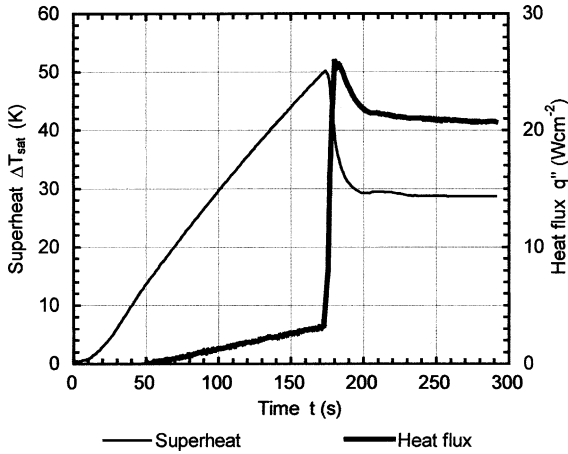


Fig. 5. Transient superheat and heat flux versus time for stepwise heat generation of 80% CHF supplied to the cartridge heaters.

power supplied at the heaters and the time derivative of sample's internal energy. For the thick flat sample, heat losses at the bottom or through lateral surfaces are quite negligible [2].

A typical example of transient behaviour for the thick flat sample is presented in Fig. 5 where time evolution of the superheat and heat flux at the wall are plotted simultaneously. The corresponding heating step is 22 Wcm^{-2} , i.e. nearly 80% of the critical heat flux.

At early stages, heat transfer is performed by convection and cell movements can be observed in the fluid upon the heating surface. The wall superheat and the heat flux transferred to the liquid increase quasi-linearly with time. The heat transfer coefficient is nearly constant. Its value equals the one measured in steady-state conditions ($h \approx 600 \text{ Wm}^{-2}\text{K}^{-1}$). Boiling starts in a quasi-explosive manner 172 s after the beginning of the step. The superheat at the wall is about 50 K and the surface heat flux of about 2.8 Wcm^{-2} . A first bubble is generated, then grows rapidly to cover the entire surface. Visualisations using a standard video camera show that its growth duration is lower than 25 ms. Okuyama et al. [3], performing transient nucleate boiling experiments on a large capacity heater (20 mm in diameter) in R-113, observed a growth duration of the initial bubble, ranging between 30 and 70 ms. After the departure of the initial bubble, nucleate boiling develops over the surface. Considering the thermocouple location and the data acquisition rate fixed in order to obtain the stability of the inverse method and the best result accuracy, transient phenomena characterised by frequencies higher than 1 Hz cannot be observed experimentally.

Comparisons with hydrophone measurements show that boiling incipience corresponds to the maximum wall superheat. Due to heat transfer enhancement associated

with boiling occurrence, wall temperature starts to decrease whereas heat flux at the wall increases. The energy stored in the sample during the natural convection regime is then released into the liquid until steady conditions are achieved. The vaporization of the overheated liquid occurring at boiling incipience when the surface superheat is greater than 40 K leads to the formation of a vapour film over the heated surface. Nevertheless the superheating of the Leidenfrost point $\Delta T_{\text{Leidenfrost}} = 132 \text{ K}$ has never been reached in the present experiments. Therefore, the temperature of the surface and thus the radiation and conduction heat transfer across the vapour film are not high enough to maintain the thin vapour film and no transition to film boiling has been observed in spite of a surface temperature greater than the one associated to the critical heat flux.

Time evolution of the wall superheat is plotted in Fig. 6 for various heating steps. About ten runs were carried out for each experimental condition. Mean values and standard deviations of the maximum wall superheat and its associated time are also presented in this figure. The wall superheat at boiling incipience increases slightly with the heat rate applied to the cartridge heaters. This tendency is relatively weak: the difference between the mean values of the wall superheat obtained for stepwise heat generation $q^* = 0.13$ and $q^* = 0.78$, is close to the standard deviation of the superheat measurement obtained for the stepwise heat generation $q^* = 0.78$.

These results can also be presented in the form of boiling curves as shown in Fig. 7. For any stepwise heat generation, heat flux transferred to the fluid during the convective regime, plotted as a function of the wall superheat, is similar to steady-state results. In this regime, heat transfer at the wall evolves in a quasi-static

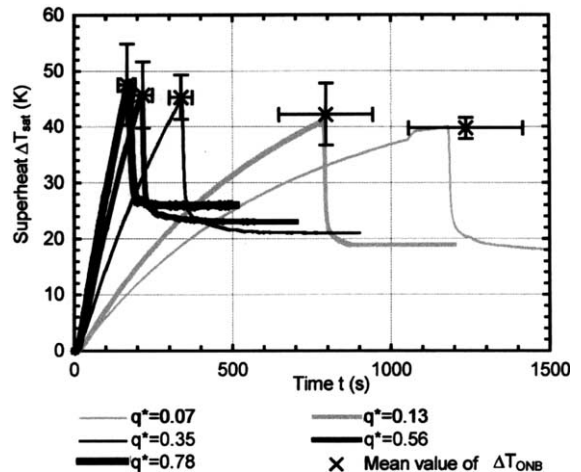


Fig. 6. Transient superheat versus time for different stepwise heat generations supplied to the cartridge heaters.

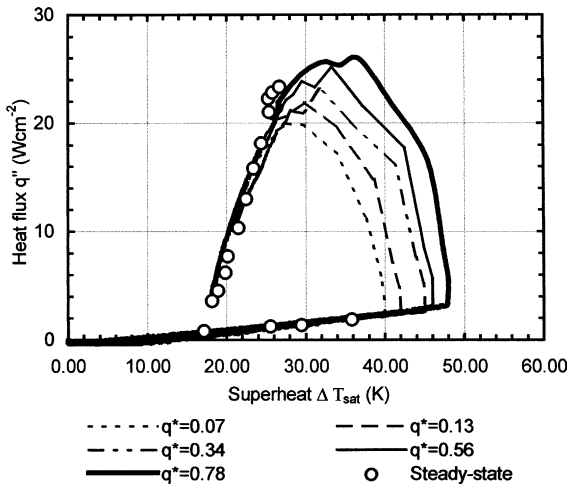


Fig. 7. Distribution of the heat flux transferred to the fluid as a function of the wall superheat.

manner due to the high thermal inertia of the sample. For any heating step, heat flux transferred to the fluid at boiling incipience ranges between 2 and 3 W cm⁻² corresponding to about 10% of the critical heat flux. Heat flux at boiling incipience is thus not significantly affected by the magnitude of the heating step supplied to the heaters.

A fast transient response follows boiling incipience leading the system in less than 3 s to a maximum heat flux value. Afterwards, time evolution of the wall heat flux and of the surface temperature are slower. Power transferred to the fluid during the transient period is greater than power supplied to the cartridge heaters. Thus heat flux transferred to the fluid can overshoot temporarily the critical heat flux. Five seconds after the onset of boiling, heat transfer at the wall evolves in a quasi-static manner. Even though these transient boiling curves look similar one with each other, a higher heating step shifts the curve to the right.

In the following part, an attempt is developed in order to connect the temperature at boiling onset with existing theories. Formation of bubbles in the superheated liquid at boiling onset may be explained either by homogeneous nucleation theory, heterogeneous nucleation theory or by activation of the pre-existing vapour nuclei trapped in cavities. The rate of formation of critical size vapour nuclei per unit volume within the bulk of a pure liquid may be estimated using the classical equation [29]:

$$J = \bar{N}_1 \left(\frac{3\sigma}{\pi m} \right)^{1/2} \exp \left[\frac{-16\pi\sigma^3}{3k_B T_1 [\eta p_{\text{sat}}(T_1) - p_1]^2} \right] \quad (7)$$

$$\text{where : } \eta = \exp \left[\frac{p_1 - p_{\text{sat}}(T_1)}{\rho_1 R_1 T_1} \right] \quad (8)$$

For organic fluids, an excellent agreement is obtained between experimental data and the superheat calculated with Eq. (7), using $J = 10^{12} \text{ m}^{-3} \text{ s}^{-1}$ [29]. The homogeneous nucleation superheat for pentane at atmospheric pressure is about 153 °C. It corresponds to a critical radius of 0.07 μm. The rate of formation of critical size vapour nuclei per unit volume changes extremely rapidly with temperature because of the exponential term in Eq. (7). Therefore, there is no probability of homogeneous nucleation in the present experimental conditions. Static contact angle for the couple pentane with a copper mirror-finished surface is about 2 [30]. For highly wetting fluids, the work of nuclei formation in heterogeneous nucleation is of the same order of magnitude as in homogeneous nucleation [31]. Thus, heterogeneous nucleation cannot be considered as being the mechanism of bubble formation in the present case. The formation of bubbles at the onset of boiling can only be explained by the activation of pre-existing gas or vapour nuclei trapped in cavities.

In the present experiments, the boiling vessel is first maintained during 4 h under a low pressure, less than 0.2 mbar, in order to degas the test section. Moreover, before each transient nucleate boiling experiment, the heater surface is maintained in vigorous boiling during 30 min. Once the cavities begin to generate bubbles, a part of the entrapped noncondensable gas that could still remain in the cavities is carried off with each bubble. The wall cavities are therefore supposed to be filled mainly with vapour. The fraction of cavities that can trap vapour decreases if the wettability of the surface increases. For highly wetting fluids such as pentane on a copper surface, only re-entrant cavities satisfying the Bankoff's criterion can trap gas or vapour, except if non-wetting local properties are present within cavities. Due to the quasi-steady conditions encountered during the convective regime, the thermal boundary layer over the heating surface is fully developed. Numerical simulations performed with the Fluent software showed that the thickness of this thermal boundary layer at the mid-radius of the surface heater is close to 5 mm. The departure diameter of bubbles in the case of pentane nucleate boiling over a copper plate is about 1.8 mm [32]. Therefore, the influence of the temperature distribution of the liquid above the cavities on the bubble growth is supposed to be insignificant during boiling incipience. According to Griffith and Wallis, onset boiling can be related to a temperature criterion using Eq. (1). Wall superheats at boiling incipience correspond, in the present case, to a cavity mouth diameter ranging between 0.3 and 0.4 μm.

The time intervals corresponding to boiling incipience (Δt_1) and to steady-state boiling development (Δt_2) are plotted in Fig. 8 for various heating steps. The time interval (Δt_1) is the difference between the time at boiling inception (t_2) and the time at heating inception

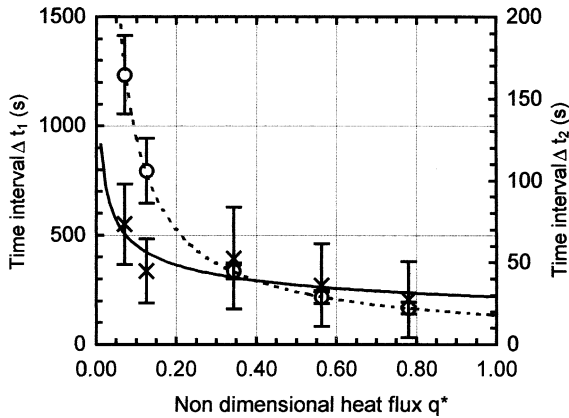


Fig. 8. Distribution of time intervals (Δt_1) and (Δt_2) as a function of the dimensionless heat flux supplied to the cartridge heaters q^* .

t_1 . The time interval (Δt_2) is the difference between the time at steady-state nucleate boiling (t_3) and the time at boiling inception (t_2). Steady-state nucleate boiling is supposed to be obtained when the time variation of the surface temperature becomes lower than 0.01 K s^{-1} . As described in a former section, the surface temperature and the heat flux transferred to the fluid at boiling incipience are not significantly affected by the heat generation condition. Therefore, the time interval (Δt_1) necessary to reach the temperature criterion for cavity activation decreases with higher heating steps.

The energy Q stored in the sample, deduced from time integration of heat flux during the convective re-

gime, is almost unaffected by a change in the heating step condition ($Q(q^* = 0.07)/Q(q^* = 0.78) = 1.2$). On the other hand, heat transfer in nucleate boiling increases significantly with the heating step ($h(q^* = 0.07) \approx 2250 \text{ W m}^{-2}\text{K}^{-1}$; $h(q^* = 0.78) \approx 8300 \text{ W m}^{-2}\text{K}^{-1}$). The transient period from boiling inception to steady state (time interval (Δt_2) in Fig. 8) corresponds principally to the release of the energy stored in the sample before boiling inception. Given some heat amount to discharge, the highest heat transfer coefficient will lead to the shortest period. Time interval for steady-state development is therefore a decreasing function of the stepwise heat flux.

4.2. Wire

Due to the very low thermal inertia of the wire, the electrical heating step is, at any time, almost integrally released in the fluid. Thereafter, the boundary condition at the wall can be considered to be a constant heating power. This is indeed a major difference with the massive heater whose boundary condition at the wall is not controlled.

Time evolution of the wire superheat is shown in Figs. 9 and 10 for various heating steps. Temperature charts appear, at first glance, to be less smooth than the ones obtained with the thick flat sample: brief events that could not be detected with the massive heater are highlighted by the wire geometry. Regardless of the heating step value, steady state finally achieved is nucleate boiling. It is therefore compliant with the stationary boiling curve presented in Fig. 4.

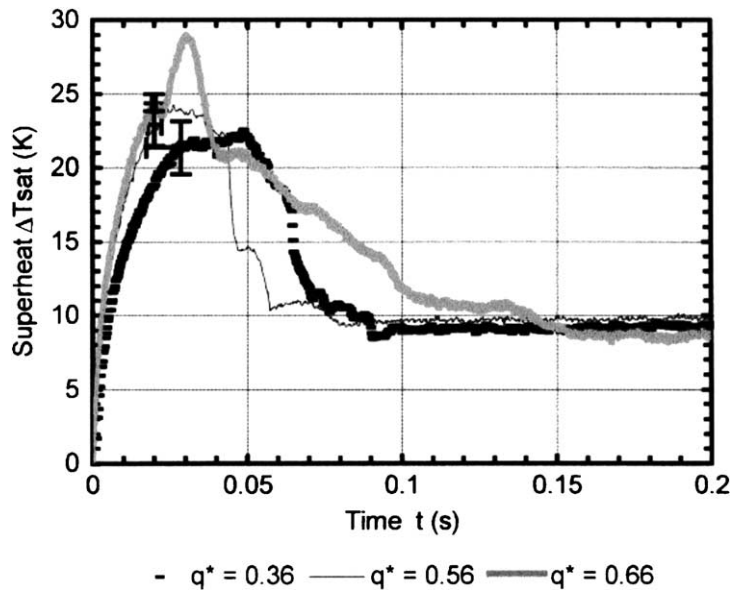


Fig. 9. Transient superheat versus time for different stepwise heat generation supplied to the wire.

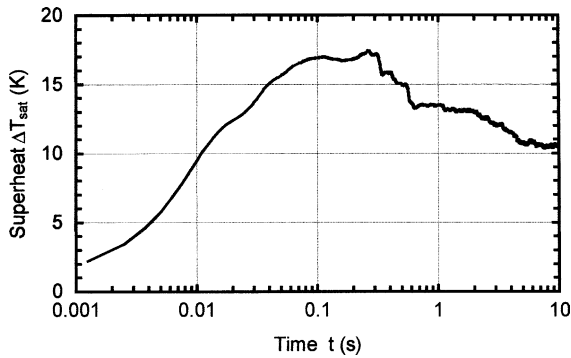


Fig. 10. Transient superheat versus time for a stepwise heat generation of $q^* = 0.04$ supplied to the wire.

At early stages, heat is released by conduction then natural convection in the liquid phase. The low efficiency of these heat transfer mechanisms leads to a rapid increase of the wire temperature. This sharp rise is stopped by the vapour onset. The wire superheat corresponding to the deviation from the curve of single phase heat transfer is identified as ΔT_{ONB} and plotted in Fig. 11 for the various heating steps. The associated time value (Δt_1) is shown in Fig. 12. Time period from boiling inception to steady state, (Δt_2), corresponds to the development of the steady nucleate boiling structure. Since any boiling event occurring on the wire changes its mean temperature, temperature charts measured for the wire are irregular. It is therefore not possible to estimate time for steady-state achievement using the same criterion as for the thick flat sample. Hence, the quantity Δt_2 is determined from visual observation and plotted in Fig. 12. From results presented in Figs. 11 and 12, it is possible to discern two different behaviours depending on heat flux.

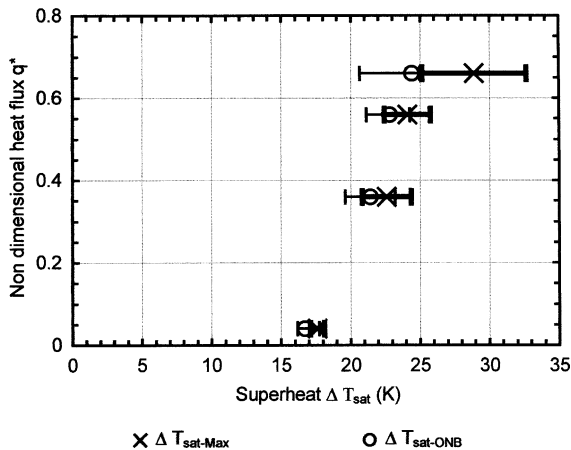


Fig. 11. Distribution of the superheat at onset boiling and the maximum superheat as a function of the dimensionless heat flux supplied to the wire q^* .

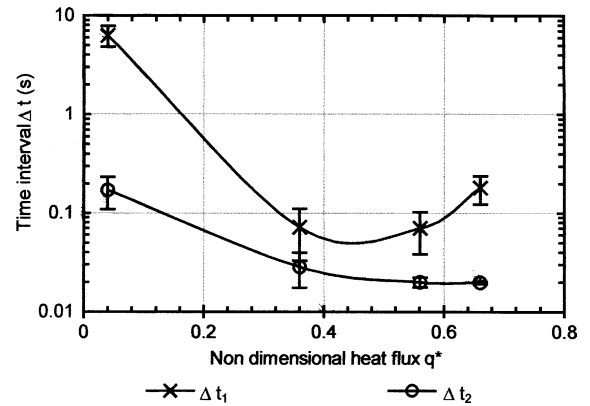


Fig. 12. Distribution of time intervals (Δt_1) and (Δt_2) as a function of the dimensionless heat flux supplied to the wire q^* .

able to discern two different behaviours depending on heat flux.

4.2.1. Low heat flux

For the lowest heating step ($q^* = 0.04$), temperature at boiling inception is comparable to the one measured in steady conditions (about 18 K as shown in Fig. 4). The temperature chart recorded for this heat flux value (Fig. 10), shows that, convection is present on the wire before boiling occurrence ($\Delta t_1 \cong 0.17$ s) since thermal plume development, associated to the end of the conductive regime, tends to flatten the temperature rise [24]. Besides, Fig. 12 shows that it takes nearly 10 s (Δt_2) to the system to achieve steady state. Then, for this low heat flux, boiling onset seems to occur similarly as in steady conditions. The pre-existing vapour nuclei trapped in cavities are activated one behind the other leading the wire temperature to a gradual decrease in time.

4.2.2. High heat flux

On the other hand, for the three highest heating steps ($q^* \geq 0.36$), temperature at boiling inception is higher than the one measured in steady conditions. The associated time value (Δt_1) is very short, as can be seen in Fig. 12. In these cases, the thermal plume is not yet fully developed. Isotherms are nearly circles and the thermal boundary layer is thinner. Since the wire may be modelled as a line heat source, i.e. as a one dimensional problem, thickness of the thermal boundary layer at boiling onset, may be estimated analytically, close to 200 μm . This value is lower than the bubble size at departure, that is about 500 μm . Bubble growth is then impeded in the upper direction. This feature contributes to a hemispherical growth, also promoted by additional factors like high wall superheat, highly wetting liquid, smooth surface with very small cavities [26].

For heating steps $q^* = 0.36$ or 0.56 , a drastic temperature drop, of several Kelvin in a few milliseconds, is observed and leads in a short while ($\Delta t_2 < 0.1$ s) to steady-state. It is now commonly accepted that such a sharp temperature decrease is the signature of micro-layer evaporation [33], usually induced by a hemispherical growth. Moreover, this temperature drop shows that many bubbles have occurred simultaneously along the wire. The wire superheat is a mean value derived from the electrical resistance of the wire; an event as visible as a temperature variation of several Kelvin in a few milliseconds represents therefore the contribution of the whole wire. Once the first bubbles have lift off, conditions for normal bubble growth are established and steady-state is achieved. This “first bubble” effect was also recently reported by Shoji and Takagi [34] performing experiments on a single conical cavity and using a high speed video camera. The authors showed that the “first bubble”, generated after a long waiting period, is characterised by a rapid horizontal growth and a large diameter, inducing a strong temperature drop at the wall. The following bubbles have an isotropic growth and some smaller dimensions. The associated temperature drop at the wall is also reduced.

Due to the simultaneous nature of this boiling onset, one may think of a nucleation process. Sinha et al. [8], comparing experimental results with Eq. (7), showed that homogeneous nucleation in liquid nitrogen under atmospheric pressure occurs for a liquid superheat close to 33 K. The associated nucleation rate J is equal to $10^{12} \text{ m}^{-3} \text{ s}^{-1}$ and the critical radius of vapour embryos is about $0.05 \text{ }\mu\text{m}$. Heterogeneous theory for smooth surfaces was implemented in the case of liquid nitrogen by Drach and Fricke [35]. They showed that temperature of heterogeneous nucleation is significantly lower than the one for homogeneous nucleation only if the contact angle is higher than 90° . Since liquid nitrogen is a highly wetting fluid, this theory can neither explain the superheat observed at boiling inception for high heating steps.

The maximum superheat observed during transients presented here, is also plotted in Fig. 11. For the three lowest heating steps, the maximum temperature is very close from that at boiling onset but does not coincide. This shows that cooling does not immediately follow the occurrence of vapour phase. For the highest heating step ($q^* = 0.66$), the maximum superheat is as high as 28 K. This is due to the formation of an insulating vapour blanket somewhere along the wire. The heat flux value is not high enough to sustain it. The vapour layer breaks off, leading the system to steady nucleate boiling. The dynamics of this boiling process slightly delays steady state achievement; time period (Δt_2) is stretched, as can be seen in Fig. 12.

5. Comparative analysis of the results and conclusion

Results reported and analysed in the former section show that the two systems present common characteristics but also some differences. The heating step values investigated in the present work all lead to steady nucleate boiling. It may be noticed that no premature transition to film boiling is observed in the present case for the thin wire. This has probably to be connected with the presence of pre-existing vapour nuclei trapped inside cavities before transient heating.

The heating condition, i.e. a stepwise heat generation, is the same for both samples. It allows to investigate the influence of thermal inertia on transient boiling. The heating step is delivered to the heating element. For the flat thick sample, the heating element are the two cartridge heaters, located at the bottom of the copper block, whereas the wire is its own heating element. The boundary condition at the wall in contact with the fluid is a constant heat flux for the thin wire while it is not controlled for the thick flat sample.

For both samples, time evolution of the wall superheat has a similar shape: a temperature overshoot is observed before steady-state achievement. Even though physical mechanisms involved in the transient process are analogous, time scales involved for both samples, are different. For the thick flat sample, except during the boiling onset period, time scales are important, in connection with the large thermal inertia of the system. Energy has first to be stored in the sample in order to increase its internal energy until its surface temperature reaches the one at boiling onset. Then, after boiling incipience, the sample has to loose a part of its internal energy to achieve a lower wall temperature, compliant with the steady nucleate boiling state. Things are similar for the wire but due to the quasi-negligible thermal inertia of the wire, time for temperature increase from the initial value to the one at boiling inception is very short. The problem may be modelled as a line heat source immersed in a liquid and submitted to a heating step. The conduction or convection problem may be solved either analytically or numerically [24]. Due to the absence of thermal inertia, time required from boiling inception to steady state, is the one required for the steady boiling structure to develop on the wall.

This study shows that during the start of a boiling system with a stepwise heat generation, the thermal behaviour and the associated time constants will be controlled by temperature at boiling inception. Moreover, this investigation shows that for the thick flat sample, even though pre-existing vapour nuclei are trapped inside the wall cavities, temperature at boiling onset is never lower than the one measured in steady conditions. A whole boiling curve has then to be described even though the system has been shut off a short while before. Since boiling onset on a massive heater is due to the

activation of pre-existing vapour nuclei, the Griffith and Wallis criterion developed for steady-state conditions is still valid for the transient case.

Besides, transient experiments conducted on the wire showed that, for very fast heating conditions, temperature at boiling onset may be higher than the one in steady conditions, despite the existence of vapour trapped in the cavities. This shows that kinetics of the liquid–vapour meniscus inside cavities plays a key role in this process. Further work has to be developed in order to explain the temperature value measured at boiling inception in this case.

Acknowledgment

This study has been performed within the framework of the french scientific network “AMETH”, dedicated to Heat Transfer Enhancement.

References

- [1] H. Auracher, W. Marquardt, Experimental studies of boiling mechanisms in all boiling regimes under steady-state and transient conditions, *Int. J. Thermal Sci.* 41 (2002) 586–598.
- [2] S. Héas, H. Robidou, M. Raynaud, M. Lallemand, Onset of transient nucleate boiling from a thick flat sample, *Int. J. Heat Mass Transfer* 46 (2003) 355–365.
- [3] K. Okuyama, Y. Lida, T. Katto, Premature transition to film boiling with stepwise heat generation 2nd report: effect of wall material and surface conditions, *Heat Transfer—Japanese Research* 25 (1996) 51–63.
- [4] H. Kawamura, F. Tachibana, M. Akiyama, Heat transfer and DNB heat flux in transient boiling, in: 4th International Heat Transfer Conference, Paris, 1970.
- [5] A. Sakurai, M. Shiotsu, Transient pool boiling heat transfer: Part 1 Incipient boiling superheat, *J. Heat Transfer* 99 (1977) 547–553.
- [6] A. Sakurai, M. Shiotsu, Transient pool boiling heat transfer: Part 2, Boiling heat transfer and burnout, *J. Heat Transfer* 99 (1977) 554–560.
- [7] O. Tsukamoto, T. Uyemura, T. Uyemura, Observation of bubble formation mechanism of liquid nitrogen subjected to transient heating, *Adv. Cryog. Eng.* 25 (1981) 476–482.
- [8] D.N. Sinha, L.C. Brodie, J.S. Semura, Liquid to vapour homogeneous nucleation in liquid nitrogen, *Phys. Rev. B* 36 (1987) 4082–4085.
- [9] K. Okuyama, Y. Lida, Transient boiling heat transfer characteristics of nitrogen bubble behavior and heat transfer rate at stepwise heat generation, *Int. J. Heat Mass Transfer* 33 (1990) 2065–2071.
- [10] M. Shiotsu, K. Hata et al., A. Sakurai, Heterogeneous spontaneous nucleation temperature on solid surface in liquid nitrogen, *Adv. Cryog. Eng.* 35 (1990) 437–445.
- [11] A. Sakurai, M. Shiotsu, K. Hata, Boiling heat transfer characteristics for heat inputs with various increasing rates in liquid nitrogen, *Cryogenics* 32 (1992) 421–429.
- [12] A. Sakurai, M. Shiotsu, K. Hata, Boiling phenomenon due to quasi-steadily and rapidly increasing heat inputs in LN₂ and LHe I, *Cryogenics* 36 (1996) 189–196.
- [13] M.-C. Duluc, G. Defresne, M.X. Fraçois, Transient boiling on thin wires in liquid nitrogen, *Adv. Cryog. Eng.* 45 (Part B) (2000) 1237–1243.
- [14] S.G. Bankoff, Ebullition from solid surface in the absence of a pre-existing gaseous phase, *Trans. ASME* 79 (1957) 735–740.
- [15] I. Thormählen, Superheating of liquids at the onset of boiling, 8th Int. Heat Transfer Conf., San Francisco 4 (1986) 2001–2006.
- [16] S.G. Bankoff, Entrapment of gas in the spreading of liquid over a rough surface, *AIChE J.* 4 (1958) 24–26.
- [17] P. Griffith, J. Wallis, The role of surface condition in nucleate boiling, *Chem. Eng. Prog. Symp. Ser.* 56 (1960) 49–63.
- [18] Y.Y. Hsu, On the size of active nucleation cavities on a heating surface, *J. Heat Transfer* 97 (1962) 207–216.
- [19] W. Tong, A. Bar-Cohen, T.W. Simon, S.M. You, Contact angle effects on boiling incipience of highly-wetting liquids, *Int. J. Heat Mass Transfer* 33 (1990) 91–103.
- [20] C.H. Wang, V.K. Dhir, On the gas entrapment and nucleation site density during pool boiling of saturated water, *J. Heat Transfer* 115 (1993) 670–679.
- [21] C.H. Wang, V.K. Dhir, Effect of surface wettability on active nucleation site density during pool boiling of water on a vertical surface, *J. Heat Transfer* 115 (1993) 659–669.
- [22] Y. Qi, J.F. Klausner, R. Mei, Role of Surface structure in heterogeneous nucleation, in: *Proceedings of the ICBHT, Montenegro Bay, Jamaica, May 4–8, 2003*, p. 10.
- [23] M. Raynaud, Influence of convection on the boiling curves of liquid nitrogen estimated round the periphery of a rotating disk, in: *Third UK National Conference, Incorporating 1st European Conference on Thermal Sciences, ETS, 1992*, pp. 147–153.
- [24] M.-C. Duluc, S. Xin, P. Le Quééré, Transient natural convection and conjugate transients around a line heat source, *Int. J. Heat Mass Transfer* 46 (2003) 341–354.
- [25] T.M. Anderson, I. Mudawar, Microelectronic cooling by enhanced pool boiling of a dielectric fluorocarbon liquid, *J. Heat Transfer* 111 (1989) 752–759.
- [26] V.P. Carey, *Liquid–Vapour Phase Change Phenomena*, Taylor & Francis, Philadelphia, 1992, pp. 167–296.
- [27] C. Corty, A.S. Foust, Surface variables in nucleate boiling, *Chem. Eng. Prog. Ser.* 17 (5) (1955) 1–12.
- [28] S.M. You, Y.S. Hong, J.P. O’Connor, The onset of film boiling on small cylinders: local dryout and hydrodynamic critical heat flux mechanisms, *Int. J. Heat Mass Transfer* 37 (1994) 2561–2569.
- [29] M. Blander, J.L. Katz, Bubble nucleation in liquids, *AIChE J.* 21 (1975) 833–848.
- [30] H.S. Liang, W.J. Yang, A remedy for hysteresis in nucleate boiling through application of micrographite fiber nucleation activator, *Exp. Heat Transfer* 9 (1996) 323–334.
- [31] R. Cole, Boiling nucleation, *Adv. Heat Transfer* 10 (1974) 85–167.
- [32] N. Ginot, S. Cioulachtjian, M. Lallemand, Analysis of the forces acting on a single bubble of n-pentane growing on a horizontal wall, in: *4th International Conference on*

- Multiphase Flow (ICMF 2001) New Orleans, May 27–June 1, 2001.
- [33] M.G. Cooper, A.J.P. Lloyd, The microlayer in nucleate pool boiling, *Int. J. Heat Mass Transfer* 12 (1969) 895–913.
- [34] M. Shoji, Y. Takagi, Bubbling features from a single artificial cavity, *Int. J. Heat Mass Transfer* 44 (2001) 2763–2776.
- [35] V. Drach, J. Fricke, Transient heat transfer from smooth surfaces in liquid nitrogen, *Cryogenics* 36 (1996) 263–269.